

Responses to reviewers

Manuscript ID: JoVE56602

submitted to

Journal of Visualized Experiments

S.Coumar and V. Lago

July 12, 2017

Letter for editor

Dear Dr. Nam Nguyen,

Please find attached a revised version of our manuscript "*Plasma actuators in rarefied super / hypersonic flows: experimental works to enhance spacecraft control and deceleration during atmospheric entries.*".

The authors would like to thank the reviewers for their time and their valuable comments. In the following pages are our point-by-point responses to the comments of the reviewers as well as your own comments. The indicated page and line numbers correspond to the revised manuscript.

We use the following color code:

- **text**: text modified or removed from the submitted version of our script
- **text**: text added in the revised version of our script

We hope that the revisions in the manuscript and our accompanying responses will be sufficient to make our manuscript suitable for publication in JOVE.

Yours sincerely,

The Authors

Editor comments

Editor's comment A: Please take this opportunity to thoroughly proofread the manuscript to ensure that there are no spelling or grammar issues. The JoVE editor will not copy-edit your manuscript and any errors in the submitted revision may be present in the published version.

Answer A: We read carefully the manuscript and corrected the spelling or grammar issues.

Editor's comment B: Please define all abbreviations before use.

Answer B: The abbreviations found on lines 36, 83, 150, 213, 222, 366 and 374 were not defined. Therefore, their definitions are put into brackets and are written close to them.

Editor's comment C: Please use focused images of uniform size/resolution (at least 300 dpi).

Answer C: We followed the recommendation of the Editor and changed the resolution of our figures to 300 dpi.

Editor's comment D: Please revise the table of the essential supplies, reagents, and equipment. The table should include the name, company, and catalog number of all relevant materials in separate columns in an xls/xlsx file.

Answer D: We filled the missing informations to complete the table.

Editor's comment E: Unfortunately, there are a few sections of the manuscript that show significant overlap with previously published work. Though there may be a limited number of ways to describe a technique, please use original language throughout the manuscript. Please see lines: 55-57, 62-67, 316-326, 339-342, 344-349, 355-372, 377-380, 456-461, 474-476.

Answer E: As it was highlighted by the Editor, even if the works are different throughout our papers, the subject remains the deceleration of reentry vehicles and thus, it is inevitable to find some similar parts. Furthermore, material and facilities used during experimental works can hardly be described in other ways. However, taking into account the Editor comment, we modified the underlined parts.

L.55-57 At typical reentry speeds, vehicles are subjected to extreme conditions and mission planning must balance three requirements: deceleration, heating management, and accuracy of the vehicle localization and velocity when landing.

to

L.55-57 The very high speeds reached by the vehicle during reentries induce extreme conditions and at least three requirements have to be fulfilled with care: deceleration, heating management, and accuracy of the vehicle localization and velocity when landing.

L.62-67 On this purpose, it has been demonstrated that plasma actuators offer the possibility to modify the shock wave shape around the vehicle and thus the drag coefficient. This could potentially reduce locally the heat flux. Compared to traditional flow control methods, plasma actuators present several advantages like their fast response time, their low weight and size and the relatively low energy consumption, offering promising applications for flight control systems at high velocities.

to

L.62-67 The plasma actuator induces an increase in the drag force on the model surface and thus, reduce the local heat flux. This effect is obtained by the modification of the shock wave shape that arises when the plasma actuator is on. Therefore, plasma actuators can be classified in the flow control methods and compared to traditional ones, their key strengths are their low weight and size and the relatively low energy consumption. So many assets that rank them as promising applications for flight control systems at high velocities.

L.316-326 This unique facility in Europe is able to reproduce a wide range of the reentry vehicles flight corridors from 140 km to 67 km of altitude. A schematic view of the facility is presented in Figure 1. It consists of three main parts: the settling chamber with a diameter of 1.3 m and a length of 2.0 m, the test chamber with a diameter of 2.3 m and a length of 5.0 m and a third chamber in which a diffuser is installed. The diffuser is connected to the pumping group through a vacuum gate. A powerful pumping group with 2 primary pumps, 2 intermediary Roots blowers and 12 Roots blowers ensures the low density flow conditions in continuous operating mode. Depending on the desired rarefaction level, the number of pumps used can be varied. When supplied with different nozzles, the wind tunnel generates subsonic, supersonic and hypersonic flows from Mach 0.8 to Mach 21, and covers a large range of Reynolds numbers from 102 up to 105 for a reference length of 100 mm (corresponding to the length of the flat plate used as model).

to

L.316-326 The MARHy wind tunnel can be equipped with a wide range of nozzles allowing the generation of subsonic, supersonic and hypersonic flows from Mach 0.8 to Mach 21, and covers a large range of Reynolds numbers from 102 up to 105 for a reference length of 100 mm (corresponding to the length of the flat plate used as model). These flow conditions reconstitute a most of the reentry vehicles flight corridors from 140 km to 67 km of altitude making this facility unique in Europe. Figure 1 exhibits the facility which can be divided in three parts: the settling chamber with a diameter of 1.3 m and a length of 2.0 m, the test chamber with a diameter of 2.3 m and a length of 5.0 m and a third chamber in which a diffuser is installed and connects the pumping group to the facility through a vacuum gate. The pumping group is composed of 2 primary pumps, 2 intermediary Roots blowers and 12 Roots blowers. Its performances makes it able to ensure low density flow conditions continuously.

L.339-342 The models are made of quartz in order to withstand the high surface temperatures reached when using the plasma actuator. The flat plates are placed in the test section, downstream the nozzle exit as sketched on Figure 3. The plasma actuator is composed of two aluminum electrodes, 50 mm-wide, 35 mm-long and 80 mm-thick.

to

L.339-342 The plasma actuator induces very high wall temperatures thus, models must be manufactured in a heat-resistant material. The flat plates are made of quartz and the position of the model in the test chamber is sketched on Figure 3. The two electrodes setting the plasma actuator are manufactured in aluminium and designed with the dimensions: 50 mm-wide, 35 mm-long and 80 μ m-thick.

L.344-349 The electrodes size is calculated in order to keep the ratio of the active electrode surface on the model surface constant and equal to 35%. The first electrode, called the active electrode or the cathode, is set at the leading edge of the plate, and is connected to a high voltage DC power supply (Spellman, SR15PN6) through a current limiting resistor ($R_s = 10.6 \text{ k}\Omega$), while the second electrode is grounded. The high voltage V_s is fixed with the power supply, which delivers the discharge current I_{HV} .

to

L.344-349 Depending on the nozzle, the core of the generated flow will have specific dimensions and the models must be adapted to these cores. Therefore, the width of the model strongly depend of the studied flow. However, in order to maintain a certain coherence, the ratio of the active electrode on the surface of the model is kept at 35%. The electrode located the closest to the leading edge is defined as the cathode or active electrode and is connected to a high voltage DC power supply (Spellman, SR15PN6) through a current limiting resistor ($R_s = 10.6 \text{ k}\Omega$), while the second electrode is grounded. The DC power supply is voltage-regulated and delivers the discharge current IHV corresponding to the chosen V_s voltage.

L.355-372 For this purpose these pressures are measured with absolute capacitive sensors (MKS, 600 series Baratron) which scales are adapted to the range of the measurement values. The manometers are connected to a MKS control unit (PR 4000B) with a 12-bit resolution. The pressure in the flow above the plate is measured with a Pitot probe connected to a MKS Baratron capacitance manometer connected to a MKS control unit (PDR-C-2C). A 3-axis traversing system, controlled by a computer, ensures the displacement of the Pitot probe with a step resolution on each axis of 0.1 mm 0.02 mm on each position. The Pitot probe is made of glass in order to avoid electrical interactions with the discharge. The Pitot tube consists of a flat-ended cylinder with an external diameter of $D = 6 \text{ mm}$ and an internal diameter of $d = 4 \text{ mm}$. The manometers positions are spotlighted on Figure 4. The flow around the flat plate is visualized with a PI-MAX Gen-II iCCD camera (1024 x 1024-pixel array) equipped with a VUV (Visible-UltraViolet) objective lens (94 mm, $f = 4.1$). The light is collected through a fluorine window located in the wall of the test section chamber as showed on Figure 4. The evolution of the surface temperature of the flat plate is monitored with an infrared thermography device. The IR device is used to measure the flat plate surface temperature during the experiments. The IR camera (FLIR ThermaCAM SC 3000) is placed on the top of the wind tunnel (see Figure 4) and focuses on the entire surface of the flat plate through a fluorine window compatible with the IR wavelength range of the camera.

to

L.355-372 Capacitive sensors (MKS, 600 series Baratron) are used to measure the stagnation pressure P_o and the static pressure P_1 and the pressure above the flat plate when combined to a Pitot probe. The Pitot tube is a flat-ended tube made of glass to avoid electrical interactions with the discharge. Its dimensions are $D = 6 \text{ mm}$ for the external diameter and $d = 4 \text{ mm}$ for the internal one. The pressure mapping above the plate is ensured with a 3-axis traversing system, controlled by a computer. The step resolution of the Pitot probe on each axis is of 0.1 mm 0.02 mm for each position. A MKS control unit (PR 4000B) with a 12-bit resolution is linked to the manometers associated to P_o and P_1 , whereas a MKS control unit (PDR-C-2C) is used for the Pitot probe acquisition. The 10V output of each MKS unit control is read by an acquisition card storing the pressures values during experiments. Figure 4 exhibits the manometers positions. A PI-MAX Gen-II iCCD camera (1024 x 1024-pixel array) equipped with a VUV (Visible-UltraViolet) objective lens (94 mm, $f = 4.1$) is used for the flow visualisation. As it is shown on figure 4, the iCCD camera is placed perpendicularly to the flow axis and collects the light through a fluorine window located in the wall of the test section chamber. An infra-red camera (FLIR ThermaCAM SC 3000) is placed on the top of the wind tunnel focusing on the model through a fluorine window compatible with the IR wavelength range of the camera. This device follows and records the live evolution of the surface temperature of the model.

L.377-380 The flow field around the flat plate is first investigated without any plasma discharge, corresponding to the study of the natural flow (namely, the baseline). The nominal operating conditions of the flow field remain those detailed in Table 1. Images obtained with the iCCD camera of the baseline flow field are presented on Figure 5.

to

L.377-380 First, the baseline is defined. It corresponds to the flow behavior around the model without any actuation. The flow conditions were detailed in Table 1. Figure 5 presents the images of the baseline recorded with the iCCD camera.

L.456-461 The temperature distributions with the infra-red camera measurements along the longitudinal axis of the plate are plotted on Figure 10. It is clear that the model surface is heated by the plasma actuator. Indeed, even if the heat source is strictly located at the cathode, the flat plate is entirely heated due to the quartz thermal conductivity. However, as the electric field varies along the X-direction, the longitudinal distribution of the surface temperature is not constant. The highest temperatures are measured close to the leading edge (i.e., above the cathode) where the electric field is the strongest and the lowest temperatures measured at the trailing edge of the flat plate.

to

L.456-461 Figure 10 displays the temperature distributions along the longitudinal axis of the model. The plots show that the plasma actuator heats the surface of the model although the distribution is non uniform and increases towards the cathode. The non-uniformity is induced by the variation of the electric field along the X-direction and this electric field is maximum close to the leading edge of the flat plate.

L.474-476 However, as it was demonstrated in previous studies, the surface heating accounted only for 50% in the shock wave angle increase; thus, it can be assumed that the percentage would be even lower in the current case with the Mach 4 flow. Consequently the purely ionization effect is predominant in this case.

to

L.474-476 However, one can assume that the ionization effect would be even higher with the Mach 4 flow than the 50% estimated in previous studies. Therefore, the influence of the surface heating on the shock wave modification will be even more negligible.

Editor's comment F: Please remove the embedded figure(s) from the manuscript. All figures should be uploaded separately to your Editorial Manager account. Each figure must be accompanied by a title and a description after the Representative Results of the manuscript text.

Answer F: We removed the embedded figures and let the linked titles.

Editor's comment G: Please remove the embedded Table from the manuscript. All tables should be uploaded separately to your Editorial Manager account in the form of an .xls or .xlsx file. Each table must be accompanied by a title and a description after the Representative Results of the manuscript text.

Answer G: We removed the embedded table and let the linked title.

Editor's comment H: Please add more details to your protocol steps. Please ensure you answer the how question, i.e., how is the step performed? Alternatively, add references to published material specifying how to perform the protocol action.

Answer H: We read with a great care the Protocol and gave any additional information that could help the Reader to understand it. When it was needed, we added references, for instance for the Pitot tube size determination and to calculate the orifice corrections.

Editor's comment I: What type of drills are used?

Answer I: In order to give the specifications of the used drill, we add this line:

L.138 For this purpose, use a diamond hollow drill of 2 mm diameter.

Editor's comment J: B2.4: What grit sandpaper?

Answer J: The grit of the sandpaper is added as follows:

Scrape the surface that will welcome the plasma actuator with sandpaper.

to

Scrape the surface that will welcome the plasma actuator with 240 grade sandpaper.

Editor's comment K: B2.5: What percentage alcohol?

Answer K: The percentage of alcohol is added as follows:

Clean with great care the model with rubbing alcohol and make sure there is no particle left on the surface.

to

Clean with great care the model with a 60 % rubbing alcohol and make sure there is no particle left on the surface.

Editor's comment L: B3.1: How thin?

Answer L: The thickness of the glue layer is added as follows:

Spread evenly a thin layer of RTV (Room Temperature Vulcanizing) glue or any other type of glue that can endure high-temperature going to at least 600C on the back of the electrodes.

to

Spread evenly a 200 micrometers thin layer of RTV (Room Temperature Vulcanizing) glue or any other type of glue that can endure high-temperature going to at least 600C on the back of the electrodes.

Editor's comment M: Please revise the text to avoid the use of any personal pronouns (e.g., "we", "you", "our" etc.).

Answer M: We removed all the personal pronouns and thus, modified the incriminated parts.

Editor's comment N: Please highlight 2.75 pages or less of the Protocol (including headings and spacing) that identifies the essential steps of the protocol for the video, i.e., the steps that should be visualized to tell the most cohesive story of the Protocol. The highlighted steps should form a cohesive narrative with a logical flow from one highlighted step to the next. Remember that non-highlighted Protocol steps will remain in the manuscript, and therefore will still be available to the reader.

Please ensure that the highlighted steps form a cohesive narrative with a logical flow from one highlighted step to the next. Please highlight complete sentences (not parts of sentences). Please ensure that the highlighted part of the step includes at least one action that is written in imperative tense.

Answer N: We highlighted the essential steps of our Protocol that should be filmed. The highlighted steps form a cohesive narrative with a logical flow and gather the main steps of our protocol to undertake experiments.

Editor's comment O: As we are a methods journal, please revise the Discussion to explicitly cover the following in detail in 3-6 paragraphs with citations:

- Critical steps within the protocol
- Any modifications and troubleshooting of the technique
- Any limitations of the technique
- The significance with respect to existing methods
- Any future applications of the technique

Answer O: Following your advice, we completely restructured the Discussion part with adding parts on the Protocol critical steps, the plasma actuators limitations and its future applications. The comparison of the plasma actuators with other existing methods was already analyzed in the Introduction part so we did not reiterate it in this part. We insert below the former Discussion part and then the modified one.

The temperature distributions with the infra-red camera measurements along the longitudinal axis of the plate are plotted on Figure 10. It is clear that the model surface is heated by the plasma actuator. Indeed, even if the heat source is strictly located at the cathode, the flat plate is entirely heated due to the quartz thermal conductivity. However, as the electric field varies along the X-direction, the longitudinal distribution of the surface temperature is not constant. The highest temperatures are measured close to the leading edge (i.e., above the cathode) where the electric field is the strongest and the lowest temperatures measured at the trailing edge of the flat plate. For a given value of IHV, the plasma discharge without the Mach 4 flow (static pressure set to 8 Pa) induced a similar heating of the flat plate (not shown here), since the temperature distribution is similar both in value and shape. This result confirms that heating of the flat plate surface is mainly related to a discharge effect and not influenced by the interaction between the Mach 4 air flow and the flat plate surface. The thermal equilibrium of the cathode temperature is reached after 1520 min; meaning that the magnitude order of the surface heating time scale is few tenth of minutes. It can be seen that the increase in surface temperature with the power discharge is not impactful. The same behavior was observed with the Mach 2 flow but with higher temperatures gradients. In rarefied flow regimes, one of the main effects expected to be responsible for the shock wave modification is the heating of the model surface. However, as it was demonstrated in previous studies, the surface heating accounted only for 50 % in the shock wave angle increase; thus, it can be assumed that the percentage would be even lower in the current case with the Mach 4 flow. Consequently the purely ionization effect is predominant in this case.

The surface heating induces a displacement effect: the flow viscosity above the heater is modified, inducing an increase in the laminar boundary layer thickness, and, consequently, the shock wave is shifted outward the flat plate surface (i.e., θ increases). This effect can be observed more clearly on Figure 11 where four Pitot pressure profiles are presented: one corresponds to the baseline, and the others correspond to the cases when different discharge powers are supplied. On the shape of the profiles measured at $X = 50$ mm, the knee geometry is found at a higher position on the Z-axis, meaning that the thickness of the boundary layer has increased and therefore, the shock wave angle too.

To demonstrate the efficiency of plasma actuators in the context of atmospheric entries, an estimation of the aerodynamic forces over the model has been made. The discussion is focused on the drag force because during atmospheric re-entries, it is directly linked with deceleration. In terms of relative variation, for a maximum wall temperature increase of almost 50%, the drag coefficient C_D is modified by +13.0% for the plasma actuation. As the main goal is to decrease the speed of a spaceship, in view to decrease the total heat, it is interesting to study the effect of the drag diminution on the heat flux over the spaceship. For the re-entry of a space shuttle in the mold of Columbia, an increase of 13% of the total drag, as estimated in this paper, corresponds to a decrease in the vehicle speed of about 7% and of about 26% of the heat flow because the heat flow is proportional to the power 3.15 of speed. Taking into account that the mass of the heat protection in the shuttle is of 9575 kg and that the decrease of the heat flow is proportional to the mass protection, 2.5 tons of the Shuttle mass could be saved with the plasma actuator.

to

The described experimental protocol presents some critical steps. The first point concerns the repeatability of experiments because for a given experimental condition, several experimental campaigns are needed. Indeed, in order to have a complete physical analysis, different diagnostics are used that cannot be applied simultaneously. This implies that the experimental set-up (model, electrodes size and shape, position of the model in the test chamber, ...) must be rigorously the same throughout the experiments. Even slight differences can induce different discharge conditions modifying the plasma actuator effects and thus, the results will not anymore be comparable. The other point directly impacts the shock wave angle measurements. Indeed, each iCCD Image needs a specific post-processing, and thus, are analyzed manually. Therefore, it is essential to apply a well-run method for every post-processing. Furthermore, the shock wave angles are also determined from Pitot probe profiles and compared to angles detected with the iCCD images to strengthen the measurements.

The technique of plasma actuators itself presents also some issues. The main limitation of such actuators is due to the flow conditions, especially the pressure and thus, the altitude of the atmospheric re-entry spacecraft. Plasma actuators have to be characterized in different flow regimes in terms of speed and pressure to extrapolate their behavior in real cases. For this purpose, it is necessary to deeply understand the plasma physics and its coupling with the flow to overcome the challenges. Some authors incriminated thermal effects (bulk and surface) for the shock waves modifications in supersonic conditions. Shin et al. investigated thermal effects with two distinct discharge modes, where an increase in the gas temperature was observed nevertheless no clear evidence of plasma effects on the flow was identified.

The present paper shows that other physical aspects due to the discharge, than thermal ones, have to be taken into account to explain the flow modifications. Figure 16 displays the temperature distributions along the longitudinal axis of the model. The plots show that the plasma actuator heats the surface of the model although the distribution is non uniform and increases towards the cathode. The non-uniformity is induced by the variation of the electric field along the X-direction and this electric field is maximum close to the leading edge of the flat plate. For a given value of the discharge current IHV, the plasma discharge without the Mach 4 flow (static pressure set to 8 Pa) induced a similar heating of the flat plate, with a temperature distribution similar (both in value and shape) to the temperature distribution when the Mach 4 flow is operating. This result confirms that the heating of the flat plate surface is mainly related to a discharge effect and not influenced by the interaction between the Mach 4 air flow and the flat plate surface. Moreover, the surface heating induces a displacement effect: the flow viscosity above the heater is modified, inducing an increase in the laminar boundary layer thickness, and consequently, the shock wave is shifted outward the flat plate surface (i.e., the shock wave angle increases). This effect can be observed more clearly on Figure 17 where four Pitot pressure profiles are presented: one corresponds to the baseline, and the others correspond to the cases when different discharge powers are supplied. On the shape of the profiles measured at $X = 50$ mm, the knee geometry is found at a higher position on the Z-axis, meaning that the thickness of the boundary layer has increased and therefore, the shock wave angle too. Experiments carried out with a Mach 2 flow and a static pressure of 8 Pa, showed that the thermal effects accounted for only 50% in the shock wave angle increase and the remain 50% were due to ionization effects. For Mach 2 and Mach 4 flows, the surface temperature distributions are similar although the temperature gradients are higher with the Mach 2 flow. Therefore, one can assume that the ionization effect would be even greater with the Mach 4 flow than the 50 % estimated in previous studies, meaning that the influence of the surface heating on the shock wave modification will be even more negligible.

During atmospheric re-entries, atmospheric drag is used to slow down the vehicle, but the amount of energy to dissipate is enormous. The rate of energy dissipation is then estimated to be proportional to the cube of the vehicle speed, inducing very high temperatures on the spacecraft which may produce serious damages if the thermal protections are not sufficient. Optimal return trajectories are designed to obtain the minimum return cost defined as the sum of the mass propellant consumed by the space vehicle to de-orbit and the mass of thermal protections. However, reduction of thermal protections could be a way to decrease the cost of future missions. For this purpose, the idea is to increase the drag force in the aim of decelerating the vehicle and the use of plasma actuators could be an alternative method. In order to estimate the efficiency of plasma actuators in heat loads reduction, numerical simulations corresponding to our experimental conditions have been carried out to determine the aerodynamic drag forces induced by the discharge over the flat plate at Mach 2 and 8 Pa. The surface heating produced by the plasma discharge is numerically simulated reproducing the shock wave angle modifications observed experimentally. Results showed that the shock wave angles with only the surface heating are

Author's comment : Some reviewers advised to improve the overall English language of the paper. Taking this in consideration, we read it again with great care and corrected all the grammar mistakes and misspellings we could find.

Response to Reviewer #1

Manuscript Summary

N/A

Major Concerns

Very important for the scientific community.

Minor Concerns

Some more details on the limitations and possible challenges would have been beneficial. The step by step narrative can be enhanced with more figures.

Manuscript Summary

N/A

Author's comment 2: Taking into consideration the Reviewer's comment, we restructured the Discussion part and added there a paragraph about the limitations faced when using plasma actuators. We hope that this will satisfy the Reviewer. We also added nine more figures to the Protocol in the aim of making the reading easier. We insert below the former Discussion part and then the modified one and the extra figures.

The temperature distributions with the infra-red camera measurements along the longitudinal axis of the plate are plotted on Figure 10. It is clear that the model surface is heated by the plasma actuator. Indeed, even if the heat source is strictly located at the cathode, the flat plate is entirely heated due to the quartz thermal conductivity. However, as the electric field varies along the X-direction, the longitudinal distribution of the surface temperature is not constant. The highest temperatures are measured close to the leading edge (i.e., above the cathode) where the electric field is the strongest and the lowest temperatures measured at the trailing edge of the flat plate. For a given value of IHV, the plasma discharge without the Mach 4 flow (static pressure set to 8 Pa) induced a similar heating of the flat plate (not shown here), since the temperature distribution is similar both in value and shape. This result confirms that heating of the flat plate surface is mainly related to a discharge effect and not influenced by the interaction between the Mach 4 air flow and the flat plate surface. The thermal equilibrium of the cathode temperature is reached after 1520 min; meaning that the magnitude order of the surface heating time scale is few tenth of minutes. It can be seen that the increase in surface temperature with the power discharge is not impactful. The same behavior was observed with the Mach 2 flow but with higher temperatures gradients. In rarefied flow regimes, one of the main effects expected to be responsible for the shock wave modification is the heating of the model surface. However, as it was demonstrated in previous studies, the surface heating accounted only for 50 % in the shock wave angle increase; thus, it can be assumed that the percentage would be even lower in the current case with the Mach 4 flow. Consequently the purely ionization effect is predominant in this case.

The surface heating induces a displacement effect: the flow viscosity above the heater is modified, inducing an increase in the laminar boundary layer thickness, and, consequently, the shock wave is shifted outward the flat plate surface (i.e., θ increases). This effect can be observed more clearly on Figure 11 where four Pitot pressure profiles are presented: one corresponds to the baseline, and the others correspond to the cases when different discharge powers are supplied. On the shape of the profiles measured at $X = 50$ mm, the knee geometry is found at a higher position on the Z-axis, meaning that the thickness of the boundary layer has increased and therefore, the shock wave angle too.

To demonstrate the efficiency of plasma actuators in the context of atmospheric entries, an estimation of the aerodynamic forces over the model has been made. The discussion is focused on the drag force because during atmospheric re-entries, it is directly linked with deceleration. In terms of relative variation, for a maximum wall temperature increase of almost 50%, the drag coefficient C_D is modified by +13.0% for the plasma actuation². As the main goal is to decrease the speed of a spaceship, in view to decrease the total heat, it is interesting to study the effect of the drag diminution on the heat flux over the spaceship. For the re-entry of a space shuttle in the mold of Columbia, an increase of 13% of the total drag, as estimated in this paper, corresponds to a decrease in the vehicle speed of about 7% and of about 26% of the heat flow because the heat flow is proportional to the power 3.15 of speed. Taking into account that the mass of the heat protection in the shuttle is of 9575 kg and that the decrease of the heat flow is proportional to the mass protection²¹, 2.5 tons of the Shuttle mass could be saved with the plasma actuator.

to

The described experimental protocol presents some critical steps. The first point concerns the repeatability of experiments because for a given experimental condition, several experimental campaigns are needed. Indeed, in order to have a complete physical analysis, different diagnostics are used that cannot be applied simultaneously. This implies that the experimental set-up (model, electrodes size and shape, position of the model in the test chamber, ...) must be rigorously the same throughout the experiments. Even slight differences can induce different discharge conditions modifying the plasma actuator effects and thus, the results will not anymore be comparable. The other point directly impacts the shock wave angle measurements. Indeed, each iCCD Image needs a specific post-processing, and thus, are analyzed manually. Therefore, it is essential to apply a well-run method for every post-processing. Furthermore, the shock wave angles are also determined from Pitot probe profiles and compared to angles detected with the iCCD images to strengthen the measurements.

The technique of plasma actuators itself presents also some issues. The main limitation of such actuators is due to the flow conditions, especially the pressure and thus, the altitude of the atmospheric re-entry spacecraft. Plasma actuators have to be characterized in different flow regimes in terms of speed and pressure to extrapolate their behavior in real cases. For this purpose, it is necessary to deeply understand the plasma physics and its coupling with the flow to overcome the challenges. Some authors incriminated thermal effects (bulk and surface) for the shock waves modifications in supersonic conditions. Shin et al. investigated thermal effects with two distinct discharge modes, where an increase in the gas temperature was observed nevertheless no clear evidence of plasma effects on the flow was identified.

The present paper shows that other physical aspects due to the discharge, than thermal ones, have to be taken into account to explain the flow modifications. Figure 16 displays the temperature distributions along the longitudinal axis of the model. The plots show that the plasma actuator heats the surface of the model although the distribution is non uniform and increases towards the cathode. The non-uniformity is induced by the variation of the electric field along the X-direction and this electric field is maximum close to the leading edge of the flat plate. For a given value of the discharge current IHV, the plasma discharge without the Mach 4 flow (static pressure set to 8 Pa) induced a similar heating of the flat plate, with a temperature distribution similar (both in value and shape) to the temperature distribution when the Mach 4 flow is operating. This result confirms that the heating of the flat plate surface is mainly related to a discharge effect and not influenced by the interaction between the Mach 4 air flow and the flat plate surface. Moreover, the surface heating induces a displacement effect: the flow viscosity above the heater is modified, inducing an increase in the laminar boundary layer thickness, and consequently, the shock wave is shifted outward the flat plate surface (i.e., the shock wave angle increases). This effect can be observed more clearly on Figure 17 where four Pitot pressure profiles are presented: one corresponds to the baseline, and the others correspond to the cases when different discharge powers are supplied. On the shape of the profiles measured at $X = 50$ mm, the knee geometry is found at a higher position on the Z-axis, meaning that the thickness of the boundary layer has increased and therefore, the shock wave angle too. Experiments carried out with a Mach 2 flow and a static pressure of 8 Pa, showed that the thermal effects accounted for only 50% in the shock wave angle increase and the remain 50% were due to ionization effects. For Mach 2 and Mach 4 flows, the surface temperature distributions are similar although the temperature gradients are higher with the Mach 2 flow. Therefore, one can assume that the ionization effect would be even greater with the Mach 4 flow than the 50 % estimated in previous studies, meaning that the influence of the surface heating on the shock wave modification will be even more negligible.

During atmospheric re-entries, atmospheric drag is used to slow down the vehicle, but the amount of energy to dissipate is enormous. The rate of energy dissipation is then estimated to be proportional to the cube of the vehicle speed, inducing very high temperatures on the spacecraft which may produce serious damages if the thermal protections are not sufficient. Optimal return trajectories are designed to obtain the minimum return cost defined as the sum of the mass propellant consumed by the space vehicle to de-orbit and the mass of thermal protections. However, reduction of thermal protections could be a way to decrease the cost of future missions. For this purpose, the idea is to increase the drag force in the aim of decelerating the vehicle and the use of plasma actuators could be an alternative method. In order to estimate the efficiency of plasma actuators in heat loads reduction, numerical simulations corresponding to our experimental conditions have been carried out to determine the aerodynamic drag forces induced by the discharge over the flat plate at Mach 2 and 8 Pa. The surface heating produced by the plasma discharge is numerically simulated reproducing the shock wave angle modifications observed experimentally. Results showed that the shock wave angles with only the surface heating are

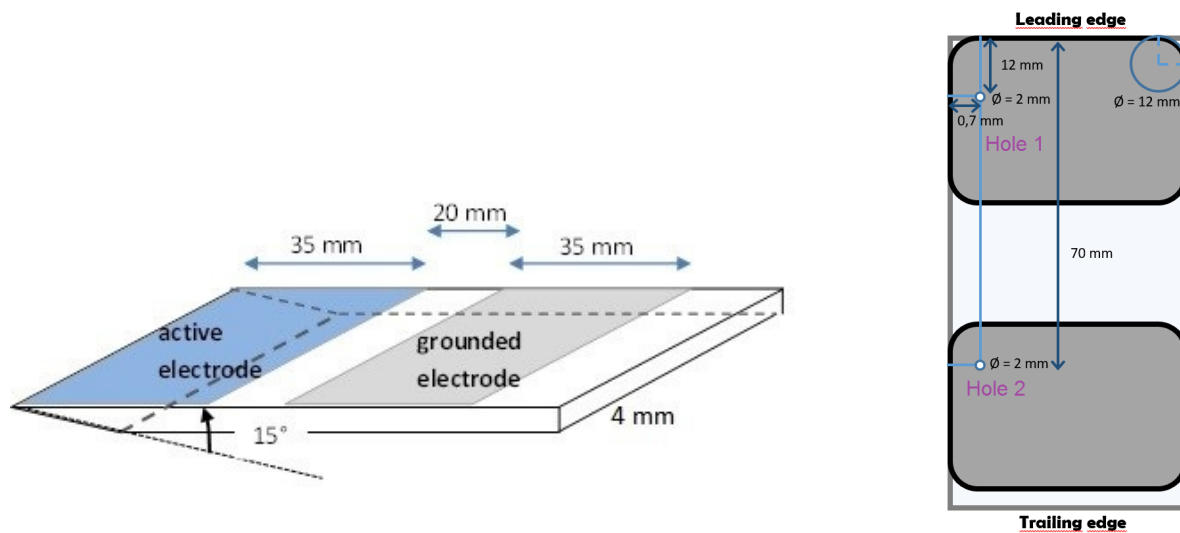


Figure 1 Figure 1 and Figure 2 of the Protocol part

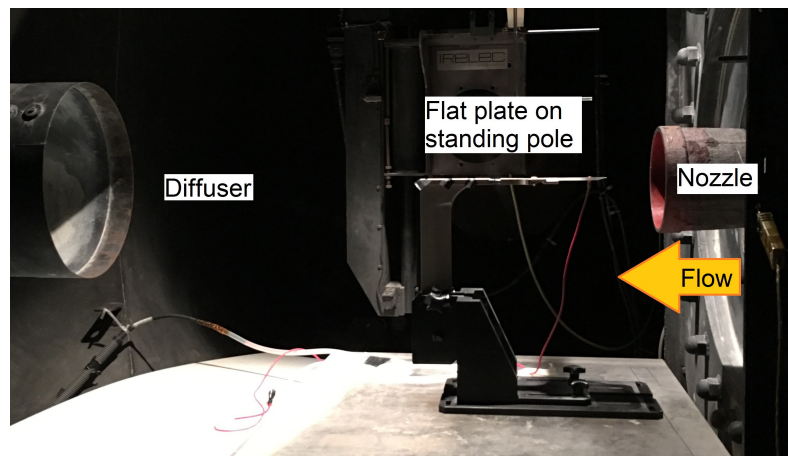
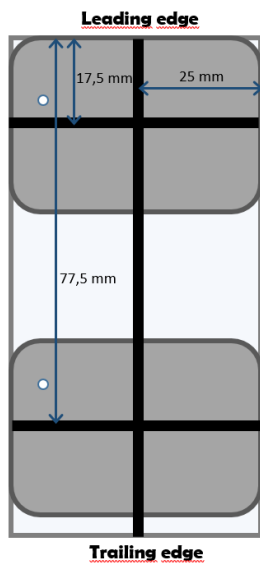


Figure 2 Figure 3 and Figure 4 of the Protocol part

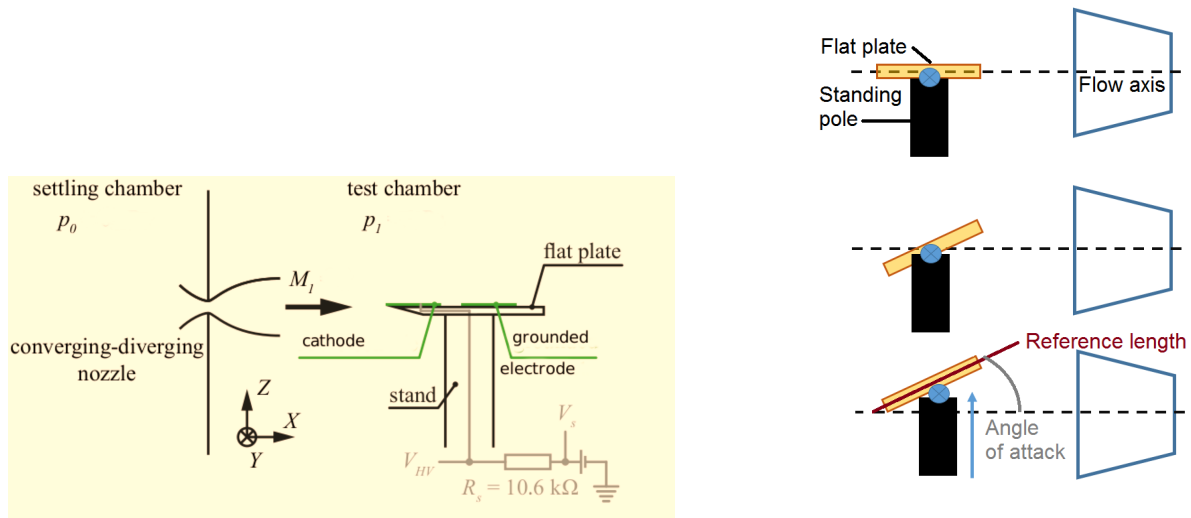


Figure 3 Figure 5 and Figure 6 of the Protocol part

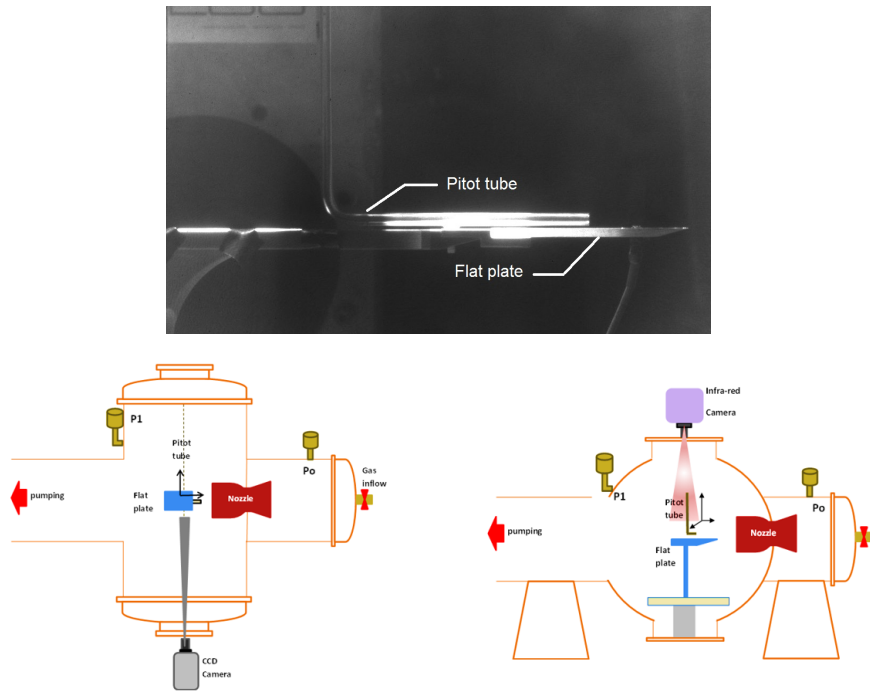


Figure 4 Figure 7 and Figure 8 of the Protocol part

Response to Reviewer 2

Manuscript Summary

The manuscript is definitely within the scope of the journal because it contains a complete test protocol and clear results. The paper could be published as-is.

Major Concerns

N/A

Minor Concerns

N/A

Manuscript Summary

N/A

Author's comment : We thank the Reviewer for its interest in our manuscript and her/his encouragements.

Response to Reviewer 3

Manuscript Summary

The draft manuscript proposes a new method for inducing drag in a Mach 4 rarefied flow (very high altitude–troposphere) as a way to soften a standard reentry. The method would use the ionization of the flow using a plasma actuator. In part, the manuscript is based on earlier work at Mach 2 [References 2 and 18] in which plasma effects become the dominant effect over thermal effects with an increase in the discharge current. In the present draft, it is recommended that Figure 5 and Figure 8 be shown side-by-side with the same flow direction along with a sketch showing the main effects. A juxtaposition as shown in Figure 7 of Reference 2 might also be considered in this regard. Although this reviewer is unfamiliar with the video concept behind this journal, I assume that the PROTOCOL's labeled A) thru G) are specifically written for this purpose. On page 7, I believe the actuator thickness should be 80 microns thick. With regard to the references, more care should be given to 2, 3, 10, and 21 to help the reader.

Major Concerns

N/A

Minor Concerns

N/A

Manuscript Summary

N/A

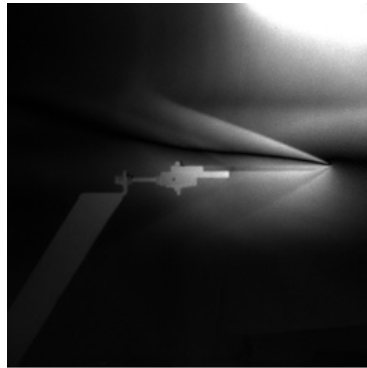
Author's comment : To make the fullest possible response, the Authors have listed the detailed comments given by the Reviewer and answered to each of the comment separately. We have also reproduced the previous and new versions, in order to highlight the modifications we made in agreement with the comments.

Reviewer comments

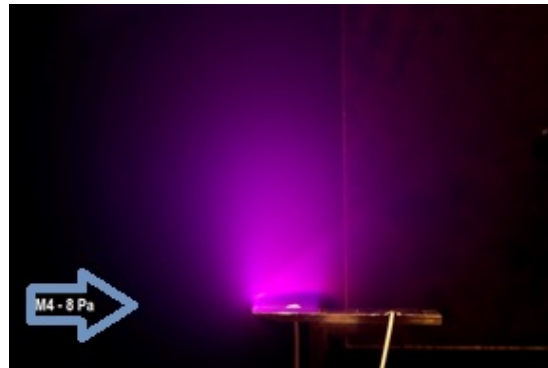
Reviewer's comment A: In the present draft, it is recommended that Figure 5 and Figure 8 be shown side-by-side with the same flow direction along with a sketch showing the main effects. A juxtaposition as shown in Figure 7 of Reference 2 might also be considered in this regard.

Answer A: We flip right to left the Figure 4 in order to get the same flow direction and we exchange the Figure 8 with another figure that shows the effect of the plasma actuator on the shock wave.

Therefore, we change these images:



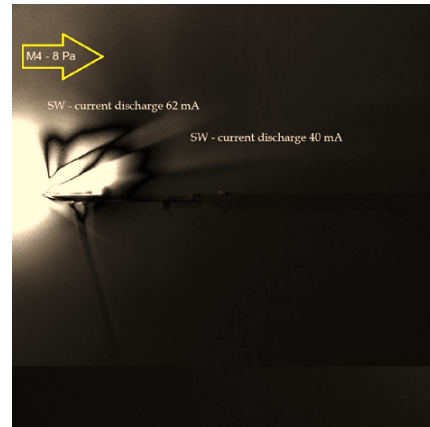
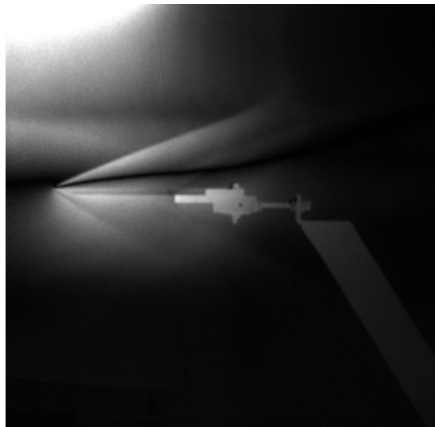
M4 / 8 Pa



M4 - 8 Pa

to these ones:

M4 / 8 Pa



Reviewer's comment B: On page 7, I believe the actuator thickness should be 80 microns thick.

Answer B: Indeed, we did a mistaken on the units and thus, we correct it as follows:

L.345-346 The plasma actuator is composed of two aluminum electrodes, 50 mm-wide, 35 mm-long and 80 mm-thick.

to

L.345-346 The two electrodes setting the plasma actuator are manufactured in aluminium and designed with the dimensions: 50 mm-width, 35 mm-length and 80 μ m-thickness.

Reviewer's comment C: With regard to the references, more care should be given to 2, 3, 10, and 21 to help the reader.

Answer C: We thank the Reviewer for this remark. Indeed we tried also to find the references with the informations we gave in the References part and were not able to find them. Therefore, we modified the references noted by the Reviewer and added more informations that were available, as for instance, the DOI numbers.

Response to Reviewer 4

Manuscript Summary

The manuscript provide details of an experimental method to utilize plasma actuator to control the flow in order to increase the drag and decrease the reentry speed. Most of the details have been provided. More detailed information about the drag should be provided to validate this technique.

Major Concerns

The language should be polished. Some description is not clear enough, which has been pointed out in the following section of the comments. The rational of the drag increase should be explained carefully since the future reader may not be familiar with plasma actuator.

Minor Concerns

See the section: Reviewer comments where each of the comments of the reviewers are listed and answered separately.

Manuscript Summary

N/A

Author's comment : To make the fullest possible response, the Authors have listed the detailed comments given by the Reviewer and answered to each of the comment separately. We have also reproduced the previous and new versions, in order to highlight the modifications we made in agreement with the comments.

Reviewer comments

Reviewer's comment A: Line 44, it should be "the mapping of the flow pressures around the model."

Answer A: Indeed, we thank the Reviewer for catching the error.

L.44-45 (...) for the mapping or the flow pressures around the model.

to

L.44-45 (...) for the mapping of the flow pressures around the model.

Reviewer's comment B: Line 55, the sentence "Aerodynamic effects..." is not clear.

Answer B: In order to clarify this sentence, we modify it.

L.56-58 Aerodynamic effects become increasingly important as the altitude decreases, and usually become dominant at 40 km, a result of the exponential increase of the air density as distance to the ground decreases.

to

L.56-58 Aerodynamic forces, as the drag and the lift, become increasingly important as the altitude decreases and usually become dominant at 40 km. It is due to the exponential increase of the air density when getting closer to the ground.

Reviewer's comment C: Line 59, it should be "Controlling the drag force is a method of..."

Answer C: As it is more elegant, we change the sentence as advised by the Reviewer.

L.60-61 Controlling the drag force is a mean of directly influencing (...)

to

L.60-61 Controlling the drag force is a method of directly influencing (...)

Reviewer's comment D: Line 79, it should be "higher than that in our experimental conditions."

Answer D: Indeed, we thank the Reviewer for catching the error.

L.81-82 (...) the use of the Schlieren technique shows that their working pressure is much higher than in our experimental condition.

to

L. 81-82 (...) the use of the Schlieren technique shows that their working pressure is much higher than that in our experimental condition.

Reviewer's comment E: Line 83, it should be "they are essentially numerical"

Answer E: Indeed, we thank the Reviewer for catching the error.

L.86-87 Other works are available but there are essentially numerical.

to

L.86-87 Other works are available but they are essentially numerical.

Reviewer's comment F: Line 90, it should be "Hence, the present work provides complementary databases and knowledge to other researchers working at higher pressure and thus higher Reynolds numbers"

Answer F: It turns out that some words of the sentence are missing and thus, the sentence is modified as advised by the Reviewer.

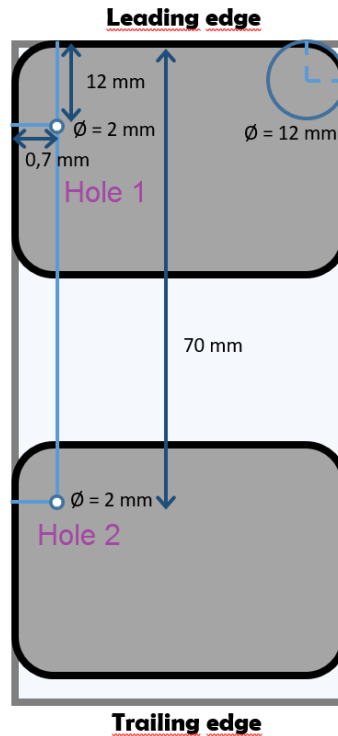
L.93-94 Hence, to bring complementary databases and knowledge with respect to other authors working at higher pressures and thus higher Reynolds number.

to

L.93-94 Hence, the present work provides complementary databases and knowledge to other researchers working at higher pressure and thus, higher Reynolds.

Reviewer's comment G: Line 120, it will be great if the author could provide a schematic of the electrode geometry indicating the radius of curvature of the rounded corner.

Answer G: We add the figure with the additional informations asked by the Reviewer. It is the Figure 2. Moreover, these required informations are added to the Protocol.



Reviewer's comment H: Line 131, it should be "trailing/leading edge angle"

Answer H: In order to five the missing information, we add it to the sentence.

p.5, L.55 Design the model (in this study, the model is beveled flat plate of 10cm-length, 5cm-width, 4mm-thickness and 15° angle).

to

p.5, L.55 Design the model (in this study, the model is beveled flat plate of 10cm-length, 5cm-width, 4mm-thickness and 15° leading edge angle).

Reviewer's comment I: Line 134 and 139, it will be more clear if the author could provide a figure showing the top view of the plate, in this figure, the dimension of the electrode and the location of the holes can be presented.

Answer I: We added the holes positions on the Figure 2. This figure has been included previously in this letter for the Comment G.

Reviewer's comment J: Line 142, it should be "This will help create roughness..."

Answer J: We thank the Reviewer for noting this grammar mistake.

L.147-148 This will help to create roughness and improve the electrode laying. In this case, the model is a beveled flat plate made in quartz.

to

L.147-148 This will help create roughness and improve the electrode laying. In this case, the model is a beveled flat plate made in quartz.

Reviewer's comment K: Line 150, "Moreover, choose glue with dilatation coefficient between those of quartz and aluminium to reduce tensions"

Answer K: The formulation given by the Reviewer is more elegant and thus, we modify the sentence.

L.155-157 Moreover chose a glue, which dilatation coefficient stands between those of the quartz and the aluminium to reduce tensions.

to

L.155-157 Moreover choose glue with dilatation coefficient between those of quartz and aluminium to reduce tensions.

Reviewer's comment L: Line 153, "Place the active electrode close to the leading edge and press it firmly to expel air bubbles. Indeed, if the air bubbles remain, they will inflate when the static pressure decreases and this will lead to detachment of the electrode."

Answer L: Again, the formulation given by the Reviewer is more elegant and thus, we modify the sentence.

L.157-159 Apply the active electrode close to the leading edge and press firmly to expel air bubbles. Indeed, if some air bubbles remain, they will inflate when lowering the pressure in the static pressure and this will lead to the detachment of the electrode.

to

L.157-159 Place the active electrode close to the leading edge and press it firmly to expel air bubbles. Indeed, if the air bubbles remain, they will inflate when the static pressure decreases and this will lead to detachment of the electrode.

Reviewer's comment M: Line 158, "Flip the flat plate over and add something heavy on top of it. This will flatten the electrodes against the flat plate."

Answer M: Again, the formulation given by the Reviewer is more elegant and thus, we modify the sentence.

L.162-163 Turn the flat plate and put on it something heavy. It will flatten the electrodes against the flat plate.

to

L.162-163 Flip the flat plate over and add something heavy on top of it. This will flatten the electrodes against the flat plate.

Reviewer's comment N: Line 162, "Use black paint, which can withstand high temperature, to draw a line along the central axis of the flat plate and two perpendicular lines passing through the center of each electrode"

Answer N: Again, the formulation given by the Reviewer is more elegant and thus, we modify the sentence.

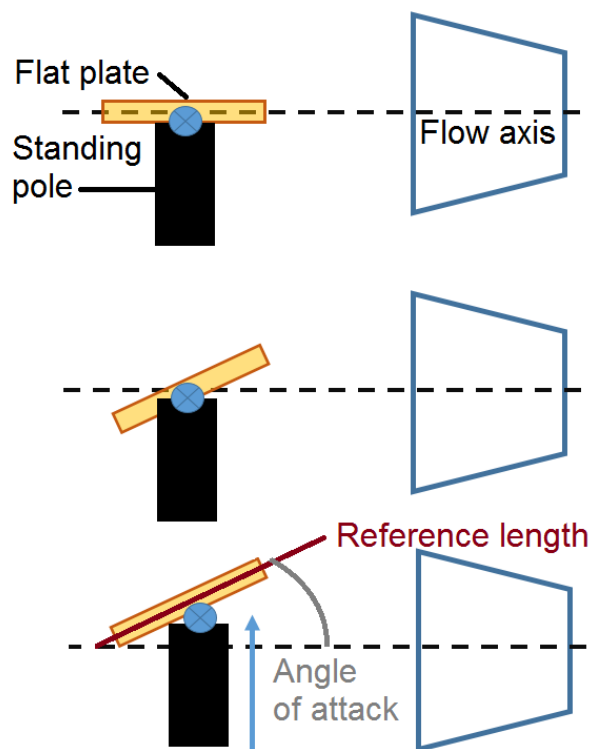
L.166-168 Draw a line following the central axis of the flat plate and two perpendicular lines passing through the center of each electrode. Use for this a black paint withstanding high temperatures.

to

L.166-168 Use black paint, which can withstand high temperature, to draw a line along the central axis of the flat plate and two perpendicular lines passing through the center of each electrode.

Reviewer's comment O: Line 175, "Set the appropriate angle of attack with the adjustment wheel. If you give an angle of attack to the flat plate adjust the height of the standing pole because the back of the flat plate must coincide with the central axis of the flow." What does this mean?

Answer O: If you angle the model, it will no more be lined up with the nozzle axis. In order, to keep some work coherence, we chose the back of the flat plate as reference point. Therefore, the standing pole height must be adjusted to make the back of the flat plate and the nozzle axis coincide. The figure below can help to get the point. However, to make clearer this part, we modify it.



L.179-181 Set the appropriate angle of attack with the adjustment wheel. If you give an angle of attack to the flat plate, adjust the height of the standing pole because the back of the flat plate must coincide with the central axis of the flow. Check that the model fits in the core of the flow.

to

L.179-181 Set the appropriate angle of attack, defined as the angle between the flow axis and the model reference length (longitudinal model axis), with an angle gauge. Therefore, the trailing edge of the model would always coincide with the flow axis. Check that the model remains in the core of the flow (see Figure 6).

Reviewer's comment P: Line 178, How to determine if the model locates in the uniform core of the jet? Probably use Pitot probe or hot-wire to determine the velocity profile?

Answer P: The flow cores have been measured in the past with Pitot profiles and before using a nozzle we have never used before, we do again some Pitot measurements and establish the profiles in the three dimensional axis without model in order to confirm the flow core size.

Reviewer's comment Q: Line 179, please provide the detailed location of the thermocouple.

Answer Q: The thermocouple is used to measure the test chamber temperature so it can be located everywhere in the test chamber, excepted in the flow. Usually, we place it opposite to the model, 30 cm from it, to make sure that it does not interfere with the flow.

L.183-184 Set a 1mm wire-diameter K-type thermocouple in the test chamber to get the static temperature.

to

L.183-184 Set a 1mm wire-diameter K-type thermocouple to get the static temperature. Place it in the test chamber opposite to the model, at least 30 cm from the model in order to avoid interactions with the flow.

Reviewer's comment R: Line 198, is there any reference which indicates how to determine the diameter of the Pitot probe?

Answer R: We add the references we use to determine the ideal Pitot diameter. Especially the paper of Potter *et al.* (1990) which allows the determination of the orifice coefficients in order to get a reasonable effect. Taking into account the orifice coefficient, we will choose a Pitot diameter as big as possible in order to keep the measurement time small enough.

- S.A Schaaf : The Pitot probe in low-density flow. AGARD, Report 525, 1966.
- J. Potter et al. : An influence of the orifice on measured pressures in rarefied flow. AEDC-TDR, 64-175, 1964.
- J. Potter et al. : Techniques Expérimentales Liées à l'Aérodynamique à Basse Densité. AGARD, Report 318 (Fr), 1990.

Reviewer's comment S: Line 210, Calibrate the Labview program meant? What does this mean?

Answer S: The word "initialize" may be more appropriate. Indeed, we have a Labview program that helps us to acquire the Pitot measurements, drive the 3-axis robot. So, before each experiment, we open the program and enter the recording parameters.

L.215 Calibrate the Labview program meant for data acquisitions for this new test session.

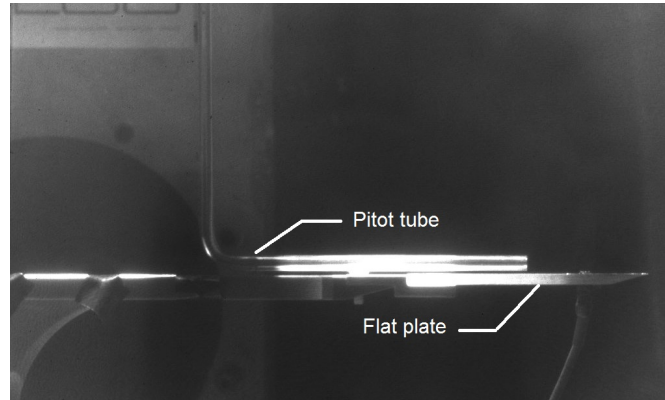
to

L.215 Initialize the Labview program meant for data acquisitions for this new test session.

Reviewer's comment T: It will be better to provide a schematic of the Pitot probe to show the structure and design.

Answer T: We added an iCCD image of the Pitot tube above the flat plate in order to help visualizing its structure. The figure is noted as the Figure 7 in the manuscript and is introduced with this sentence.

L.364-366 (...) (see Figure 7 that shows the Pitot tube above the flat plate at position $X = 50$ mm, $Y = 0$ mm, $Z = 0$ mm which, corresponds to the middle of the flat plate)



Reviewer's comment U: Line 226, How to estimate the emissivity of the painted electrode.

Answer U: We gave the method in the manuscript but it was not complete, therefore, we modify the part dedicated to the paint emissivity.

L.231-233 3.3 Estimate the emissivity of the painted electrode ε by measuring the surface temperature simultaneously with both the IR camera and a K-type thermocouple flush mounted on the flat plate surface.

to

L.231-233 3.3 Measure the surface temperature simultaneously with both the IR camera and a K-type thermocouple flush mounted on the flat plate surface. The temperature measured by the IR camera may differ from the one measured by the thermocouple as the initial calibration of the camera sets the emissivity ε at 1. If so, estimate the real emissivity of the black paint, as the ratio of the temperature given by the thermocouple on the temperature given by the IR camera.

3.4 Apply the real emissivity to the IR camera calibration to obtain the real surface temperatures with this device.

3.5 Set the good sensibility range of the camera according to the expected results during the test.

Reviewer's comment V: Line 390, any explanation on the difference between the experimental data and the numerical simulation?

Answer V: The boundary layer shape is not well reproduced by the simulation which suggests that for the DISIRAF code has to be improved in order to reproduce in a better way the shock wave for high Mach numbers. However, the z-position of the pressure peak is coherent with the numerical plot and this is precisely what was expecting when doing the simulations, in order to validate the experimental shock wave angles values.

Reviewer's comment W: Line 483 to Line 495, This paragraph should be the most important section of this article since the objective of the experiment discussed in present communication is to utilizing the plasma actuator to increase the drag and decrease the reentry speed of the vehicle. Some direct comparison of the drag and reentry

speed between the case with and without the plasma actuator should be presented in this section, using either table or figure. The drag should be determined by experimental method or estimated based on velocity or pressure data. The detail should be provided.

Answer W: Following your advice, we completely restructured the Discussion part with adding parts on the Protocol critical steps, the plasma actuators limitations and its future applications. We also enhanced the drag discussion and added two figures to illustrate the method for the drag estimation. One explains how we found an empirical law relating the shock wave angle and the drag coefficient and the other one presents the space shuttle re-entry guidance in terms of drag acceleration, as a function of the relative velocity, for the real trajectory and for the trajectory with an increase of 13 % for the drag coefficient. We hope that this new discussion answers your comments.

The temperature distributions with the infra-red camera measurements along the longitudinal axis of the plate are plotted on Figure 10. It is clear that the model surface is heated by the plasma actuator. Indeed, even if the heat source is strictly located at the cathode, the flat plate is entirely heated due to the quartz thermal conductivity. However, as the electric field varies along the X-direction, the longitudinal distribution of the surface temperature is not constant. The highest temperatures are measured close to the leading edge (i.e., above the cathode) where the electric field is the strongest and the lowest temperatures measured at the trailing edge of the flat plate. For a given value of IHV, the plasma discharge without the Mach 4 flow (static pressure set to 8 Pa) induced a similar heating of the flat plate (not shown here), since the temperature distribution is similar both in value and shape. This result confirms that heating of the flat plate surface is mainly related to a discharge effect and not influenced by the interaction between the Mach 4 air flow and the flat plate surface. The thermal equilibrium of the cathode temperature is reached after 1520 min; meaning that the magnitude order of the surface heating time scale is few tenth of minutes. It can be seen that the increase in surface temperature with the power discharge is not impactful. The same behavior was observed with the Mach 2 flow but with higher temperatures gradients. In rarefied flow regimes, one of the main effects expected to be responsible for the shock wave modification is the heating of the model surface. However, as it was demonstrated in previous studies, the surface heating accounted only for 50 % in the shock wave angle increase; thus, it can be assumed that the percentage would be even lower in the current case with the Mach 4 flow. Consequently the purely ionization effect is predominant in this case.

The surface heating induces a displacement effect: the flow viscosity above the heater is modified, inducing an increase in the laminar boundary layer thickness, and, consequently, the shock wave is shifted outward the flat plate surface (i.e., θ increases). This effect can be observed more clearly on Figure 11 where four Pitot pressure profiles are presented: one corresponds to the baseline, and the others correspond to the cases when different discharge powers are supplied. On the shape of the profiles measured at $X = 50$ mm, the knee geometry is found at a higher position on the Z-axis, meaning that the thickness of the boundary layer has increased and therefore, the shock wave angle too.

To demonstrate the efficiency of plasma actuators in the context of atmospheric entries, an estimation of the aerodynamic forces over the model has been made. The discussion is focused on the drag force because during atmospheric re-entries, it is directly linked with deceleration. In terms of relative variation, for a maximum wall temperature increase of almost 50%, the drag coefficient C_D is modified by +13.0% for the plasma actuation. As the main goal is to decrease the speed of a spaceship, in view to decrease the total heat, it is interesting to study the effect of the drag diminution on the heat flux over the spaceship. For the re-entry of a space shuttle in the mold of Columbia, an increase of 13% of the total drag, as estimated in this paper, corresponds to a decrease in the vehicle speed of about 7% and of about 26% of the heat flow because the heat flow is proportional to the power 3.15 of speed. Taking into account that the mass of the heat protection in the shuttle is of 9575 kg and that the decrease of the heat flow is proportional to the mass protection, 2.5 tons of the Shuttle mass could be saved with the plasma actuator.

to

The described experimental protocol presents some critical steps. The first point concerns the repeatability of experiments because for a given experimental condition, several experimental campaigns are needed. Indeed, in order to have a complete physical analysis, different diagnostics are used that cannot be applied simultaneously. This implies that the experimental set-up (model, electrodes size and shape, position of the model in the test chamber, ...) must be rigorously the same throughout the experiments. Even slight differences can induce different discharges conditions modifying the plasma actuator effects and thus, the results will not anymore be comparable. The other point directly impacts the shock wave angle measurements. Indeed, each iCCD Image needs a specific post-processing, and thus, are analyzed manually. Therefore, it is essential to apply a well-run method for every post-processing. Furthermore, the shock wave angles are also determined from Pitot probe profiles and compared to angles detected with the iCCD images to strengthen the measurements.

The technique of plasma actuators itself presents also some issues. The main limitation of such actuators is due to the flow conditions, especially the pressure and thus, the altitude of the atmospheric re-entry spacecraft. Plasma actuators have to be characterized in different flow regimes in terms of speed and pressure to extrapolate their behavior in real cases. For this purpose, it is necessary to deeply understand the plasma physics and its coupling with the flow to overcome the challenges. Some authors incriminated thermal effects (bulk and surface) for the shock waves modifications in supersonic conditions. Shin et al. investigated thermal effects with two distinct discharge modes, where an increase in the gas temperature was observed nevertheless no clear evidence of plasma effects on the flow was identified.

The present paper shows that other physical aspects due to the discharge, than thermal ones, have to be taken into account to explain the flow modifications. Figure 16 displays the temperature distributions along the longitudinal axis of the model. The plots show that the plasma actuator heats the surface of the model although the distribution is non uniform and increases towards the cathode. The non-uniformity is induced by the variation of the electric field along the X-direction and this electric field is maximum close to the leading edge of the flat plate. For a given value of the discharge current IHV, the plasma discharge without the Mach 4 flow (static pressure set to 8 Pa) induced a similar heating of the flat plate, with a temperature distribution similar (both in value and shape) to the temperature distribution when the Mach 4 flow is operating. This result confirms that the heating of the flat plate surface is mainly related to a discharge effect and not influenced by the interaction between the Mach 4 air flow and the flat plate surface. Moreover, the surface heating induces a displacement effect: the flow viscosity above the heater is modified, inducing an increase in the laminar boundary layer thickness, and consequently, the shock wave is shifted outward the flat plate surface (i.e., the shock wave angle increases). This effect can be observed more clearly on Figure 17 where four Pitot pressure profiles are presented: one corresponds to the baseline, and the others correspond to the cases when different discharge powers are supplied. On the shape of the profiles measured at $X = 50$ mm, the knee geometry is found at a higher position on the Z-axis, meaning that the thickness of the boundary layer has increased and therefore, the shock wave angle too. Experiments carried out with a Mach 2 flow and a static pressure of 8 Pa, showed that the thermal effects accounted for only 50% in the shock wave angle increase and the remain 50% were due to ionization effects. For Mach 2 and Mach 4 flows, the surface temperature distributions are similar although the temperature gradients are higher with the Mach 2 flow. Therefore, one can assume that the ionization effect would be even greater with the Mach 4 flow than the 50 % estimated in previous studies, meaning that the influence of the surface heating on the shock wave modification will be even more negligible.

During atmospheric re-entries, atmospheric drag is used to slow down the vehicle, but the amount of energy to dissipate is enormous. The rate of energy dissipation is then estimated to be proportional to the cube of the vehicle speed, inducing very high temperatures on the spacecraft which may produce serious damages if the thermal protections are not sufficient. Optimal return trajectories are designed to obtain the minimum return cost defined as the sum of the mass propellant consumed by the space vehicle to de-orbit and the mass of thermal protections. However, reduction of thermal protections could be a way to decrease the cost of future missions. For this purpose, the idea is to increase the drag force in the aim of decelerating the vehicle and the use of plasma actuators could be an alternative method. In order to estimate the efficiency of plasma actuators in heat loads reduction, numerical simulations corresponding to our experimental conditions have been carried out to determine the aerodynamic drag forces induced by the discharge over the flat plate at Mach 2 and 8 Pa. The surface heating produced by the plasma discharge is numerically simulated reproducing the shock wave angle modifications observed experimentally. Results showed that the shock wave angles with only the surface heating are

Conclusions

The authors have applied a special care to answer to general remarks and questions of the reviewers. The Introduction section has been entirely modified, we added references in order to answer to the lack of information revealed by the reviewers. Other sections have been revised to agree with the reviewers comments. We hope that this revised version of our paper will satisfy attempts of the reviewers and the editor.

Finally, the authors thank the reviewers for their helpful reviewing and their constructive comments. It will be notified in acknowledgments as

... The authors would furthermore like to acknowledge the constructive feedback from the reviewers.

Yours sincerely,

The Authors